

# Structure of an Electron Transfer Complex: Methylamine Dehydrogenase, Amicyanin, and Cytochrome $c_{551i}$

Longyin Chen, Rosemary C. E. Durley, F. Scott Mathews,\*  
Victor L. Davidson

The crystal structure of a ternary protein complex has been determined at 2.4 angstrom resolution. The complex is composed of three electron transfer proteins from *Paracoccus denitrificans*, the quinoprotein methylamine dehydrogenase, the blue copper protein amicyanin, and the cytochrome  $c_{551i}$ . The central region of the  $c_{551i}$  is folded similarly to several small bacterial c-type cytochromes; there is a 45-residue extension at the amino terminus and a 25-residue extension at the carboxyl terminus. The methylamine dehydrogenase-amicyanin interface is largely hydrophobic, whereas the amicyanin-cytochrome interface is more polar, with several charged groups present on each surface. Analysis of the simplest electron transfer pathways between the redox partners points out the importance of other factors such as energetics in determining the electron transfer rates.

Electron transfer is central to bioenergetic processes such as respiration, photosynthesis, and many oxidation-reduction reactions in intermediary metabolism. Biological electron transfer may occur between protein-bound prosthetic groups separated by long distances, often greater than 10 Å, and displays high efficiency and specificity (1, 2). Although extensively studied, the mechanism and control of electron transfer within protein systems is not well understood. Most electron transfer chains contain integral membrane proteins that are difficult to purify, crystallize, and study in solution. Methylamine dehydrogenase (MADH), amicyanin, and cytochrome  $c_{551i}$ , all from *Paracoccus denitrificans*, form a soluble electron transfer chain of proteins, and because they are soluble it has been possible to examine their structures and study their interactions.

MADH (E.C. 1.4.99.3) is an inducible, periplasmic enzyme that is present in several methylotrophic and autotrophic bacteria (3). It catalyzes the oxidative deamination of primary amines to the respective aldehydes. MADH (126 kD) from *P. denitrificans* is a heterotetramer consisting of two heavy (H) and two light (L) subunits (4). The redox cofactor of MADH is tryptophan tryptophylquinone (TTQ) (5), which is derived from two posttranslationally modified tryptophan residues that have been covalently linked through their indole rings. One of these

tryptophans also has been converted to an orthoquinone, which participates in the catalytic reaction of the enzyme. The physiological electron acceptor for MADH is amicyanin (11.5 kD), a cupredoxin (6); the structure of a binary complex between MADH and amicyanin has been described (7). In vitro experiments (8) show that electrons can be transferred from amicyanin to cytochrome  $c_{551i}$  (17.5 kD), which contains 155 amino acids and one heme group and is induced during

growth on methylamine or on methanol. The electrons are ultimately donated to the membrane-bound cytochrome oxidase.

We have reported the crystallization and preliminary analysis of a ternary complex between MADH, amicyanin, and cytochrome  $c_{551i}$  and of the isomorphous complex containing the copper-free apoamicyanin (9). The polypeptide chain of the cytochrome  $c_{551i}$  molecule has now been traced, with the exception of eight COOH-terminal residues. The phases used for the initial chain tracing were derived after partial refinement of the MADH, amicyanin, and heme portions of the complex. Several stages of model building and refinement, including an omit map with the simulated annealing procedure of X-PLOR (10), were carried out in order to trace the entire cytochrome. The refined model of the apoamicyanin ternary complex has an R factor of 0.179 in the resolution range 12.0 to 2.4 Å, with root mean square (rms) deviations from ideal bond distances and angles of 0.017 Å and 3.58°, respectively. The model, consisting of one heterotetramer within the asymmetric unit, contains 5805 protein atoms, one heme group, 127 solvent molecules, and one phosphate (11).

The ternary complex (Fig. 1) consists of two HLAC (heavy chain, light chain, amicyanin, cytochrome) heterotetramers re-

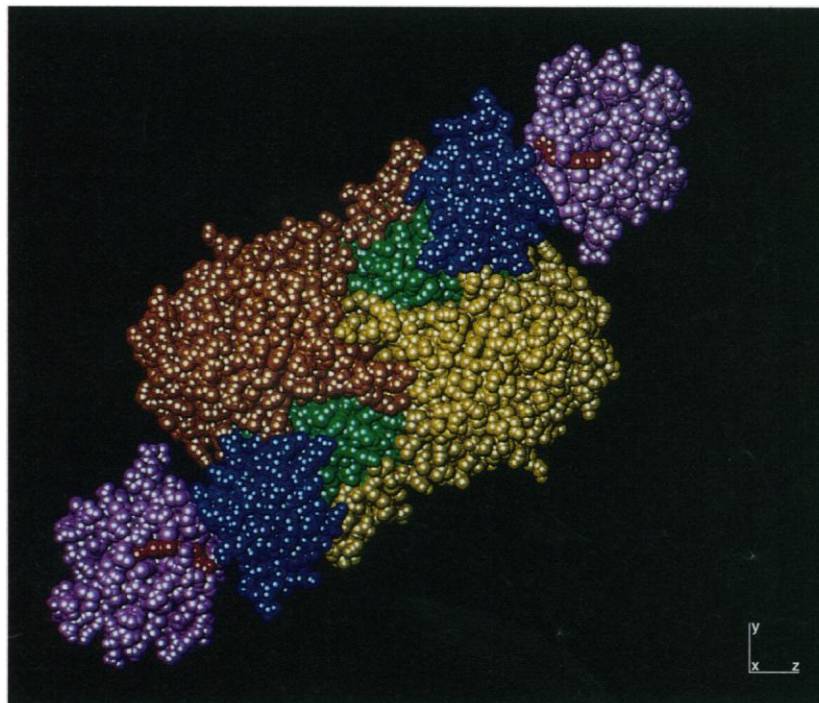


**Fig. 1.** Space-filling model of the (HLAC)<sub>2</sub> octamer. The colors are assigned as follows: yellow and brown for the two H subunits, green for the L subunit, blue for amicyanin, purple for cytochrome, and red for TTQ and for the heme group of the cytochrome, which appears partially exposed (25).

L. Chen, R. C. E. Durley, F. S. Mathews, Department of Biochemistry and Molecular Biophysics, Washington University School of Medicine, St. Louis, MO 63110, USA.

V. L. Davidson, Department of Biochemistry, University of Mississippi Medical Center, Jackson, MS 39216, USA.

\*To whom correspondence should be addressed.

lated by a molecular twofold axis that is coincident with a crystallographic twofold axis parallel to the *a* axis. In the model, the H subunit consists of 373 residues (1 to 373), and the L subunit contains 125 residues (7 to 131), which include the TTQ moiety. The model for amicyanin consists of all 105 residues plus a copper atom, and the cytochrome model consists of 147 residues and the heme group.

Amicyanin is in contact with both MADH and the cytochrome in the ternary complex. The association between amicyanin and MADH is very similar to that observed in the binary complex (7), involving both the H and L subunits of MADH. The distance from the C<sup>n</sup>2 atom of Trp<sup>57</sup> from the L subunit of MADH, where substrate oxidation is believed to occur (12), to the copper atom of amicyanin is 15.8 Å. The distance from the surface-exposed edge of Trp<sup>108</sup> to the center of the copper atom is 9.4 Å. The cytochrome molecule is also adjacent to amicyanin, but is separated from both the H and L subunits of MADH within each HLAC tetramer. The iron of the heme group and the copper of amicyanin are 24.8 Å apart. Within the complex, the subunits L, A, and C sit in a row, with the atom C<sup>n</sup>2 of Trp<sup>57</sup> separated from the iron atom by 40.1 Å. This linear arrangement of the three proteins, with no contact between cytochrome *c*<sub>551i</sub> and MADH, is consistent with the observation that no direct electron transfer occurred in solution between these two proteins without the presence of amicyanin (8).

Cytochrome *c*<sub>551i</sub> (Fig. 2) contains five  $\alpha$  helices, the central three of which envelop the heme group and correspond to analogous helices in eukaryotic and most other prokaryotic c-type cytochromes, which share the "cytochrome c-fold" (13). The heme-binding sequence Cys<sup>57</sup>-Ser<sup>58</sup>-Gly<sup>59</sup>-Cys<sup>60</sup>-His<sup>61</sup> forms the end of helix II, which is kinked at Cys<sup>57</sup>, and bends around the edge of the heme group toward His<sup>61</sup>. Helix III lies within the polypeptide chain segment connecting the two iron ligands, His<sup>61</sup> and Met<sup>101</sup>. The heme group shows significant puckering (Fig. 3). In the isolated cytochrome structure (14), the heme group is partially exposed to solvent at two places. At the left side of the molecule, as shown in Fig. 2, the vinyl and methylene carbon atoms on pyrrole ring C are exposed, whereas at the back the methyl and part of the propionate chain on pyrrole ring D are exposed. This partially exposed propionate is within 6.9 Å of the amicyanin-cytochrome interface.

Cytochrome *c*<sub>551i</sub> is highly acidic, with 27 acidic residues (12 Asp and 15 Glu) and only 8 basic residues (5 Lys and 3 Arg) in the molecule. Two charged residues, Asp<sup>86</sup> and Arg<sup>115</sup>, are buried in the interior of the

protein and form a salt bridge connecting helices III and IV. The remaining charged residues are located on the surface of the molecule. However, these charged residues are not distributed evenly over the surface, but are located mostly on the right side of the molecule (Fig. 2), away from the heme group and its hydrophobic surroundings.

Within the MADH-amicyanin interface (Fig. 4) the change in solvent-accessible surface area (15) upon complex formation is  $-715 \text{ \AA}^2$  for MADH and  $-770 \text{ \AA}^2$  for amicyanin (obtained by comparing the complex to the isolated components). Twenty-five residues of MADH (8 in the H subunit and 17 in the L subunit) are associated with the interface. Of these, 16

residues are hydrophobic and only 5 are charged (2 in H and 3 in L). Likewise, 20 residues of amicyanin are involved in the interface, 4 charged, 5 neutral, and 11 hydrophobic. The interface is therefore quite hydrophobic, despite the presence of nine charged residues (Asp, Glu, Lys, Arg) and nine neutral hydrophilic residues (Asn, Gln, Ser, Thr, Tyr, His). There is one strong salt bridge (2.7 Å separation, partially buried) connecting the H subunit and one weak salt bridge (4.4 Å separation, solvent accessible) connecting the L subunit to amicyanin. In addition, three solvent molecules bridge MADH and amicyanin. Of the remaining charged groups within the interface, one pair forms a partially

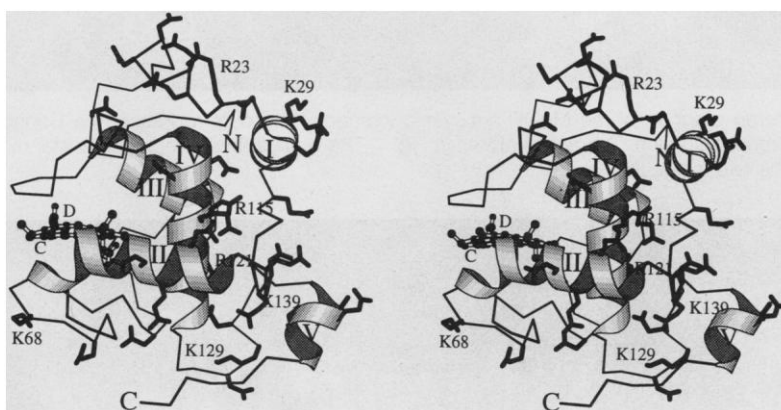


**Fig. 2.** Stereo diagram of cytochrome *c*<sub>551i</sub>. The five  $\alpha$  helices, represented by coils, are labeled in Roman numerals. Helix II (residues 46 to 61), helix III (residues 86 to 96), and helix IV (residues 110 to 124) are packed around the heme group, with helices II and IV nearly perpendicular to each other. The surfaces of the molecules, where pyrrole rings C and D are partially exposed to solvent, are on the left and the rear of the diagram, respectively. Twenty-five of the 8 basic side chains are included as heavy lines, with the basic side chains labeled; the remaining acidic and basic side chains are contained in the peptide segment 148–155, which is disordered. This diagram was made with the program MOLSCRIPT (26).

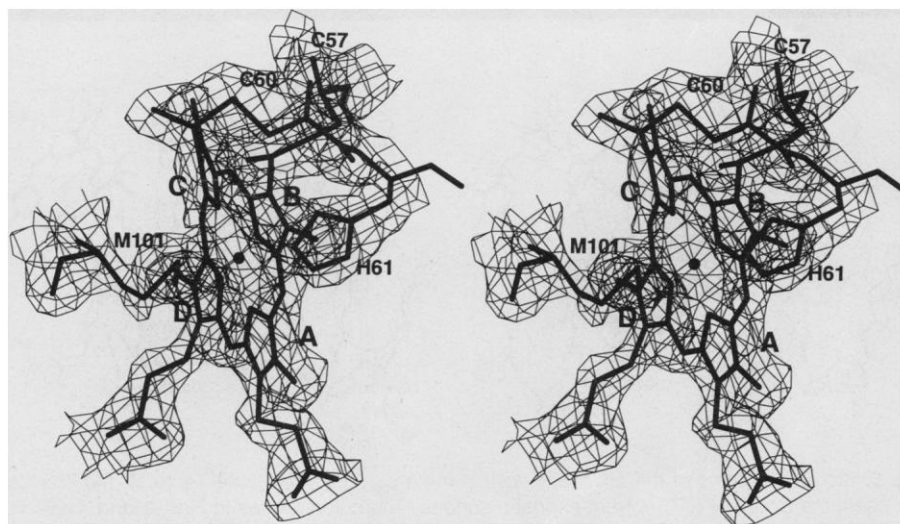


**Fig. 3.** Stereo diagram of the heme group superimposed on the electron density (contoured at 1.2 $\sigma$ ). The electron density map was computed with  $(2F_o - F_c)$  as Fourier coefficients, where  $F_o$  and  $F_c$  are the observed and the calculated structure factors on the basis of the final refined model. The four heme ligands and pyrrole rings A to D are indicated.

buried salt bridge on the surface of MADH (linking the H and L subunits) and the others are directed into solution or form intramolecular hydrogen bonds.

Likewise, the neutral hydrophilic residues point into solution or form intramolecular hydrogen bonds.

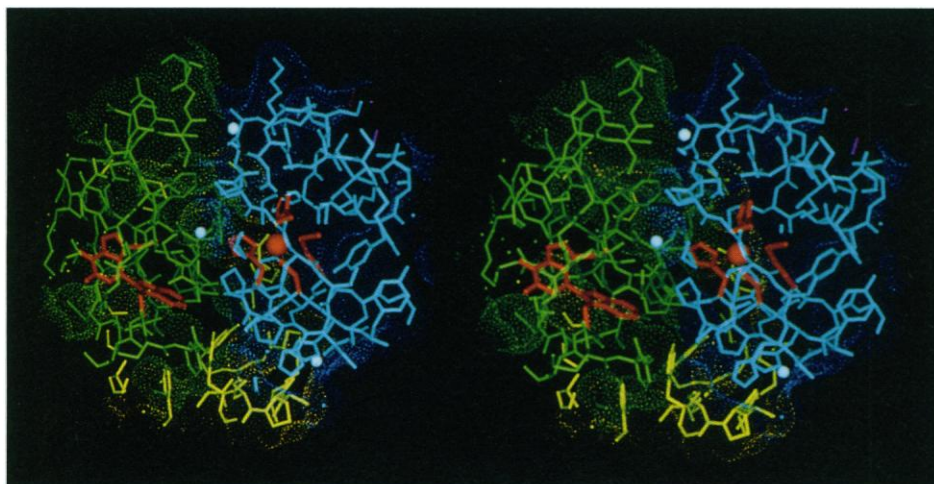


**Fig. 4.** Stereo diagram of the MADH-amicyanin interface. The dots represent the Connolly (27) solvent-exposed surface. The colors are as in Fig. 1. The white spheres represent water molecules that link the two molecules.

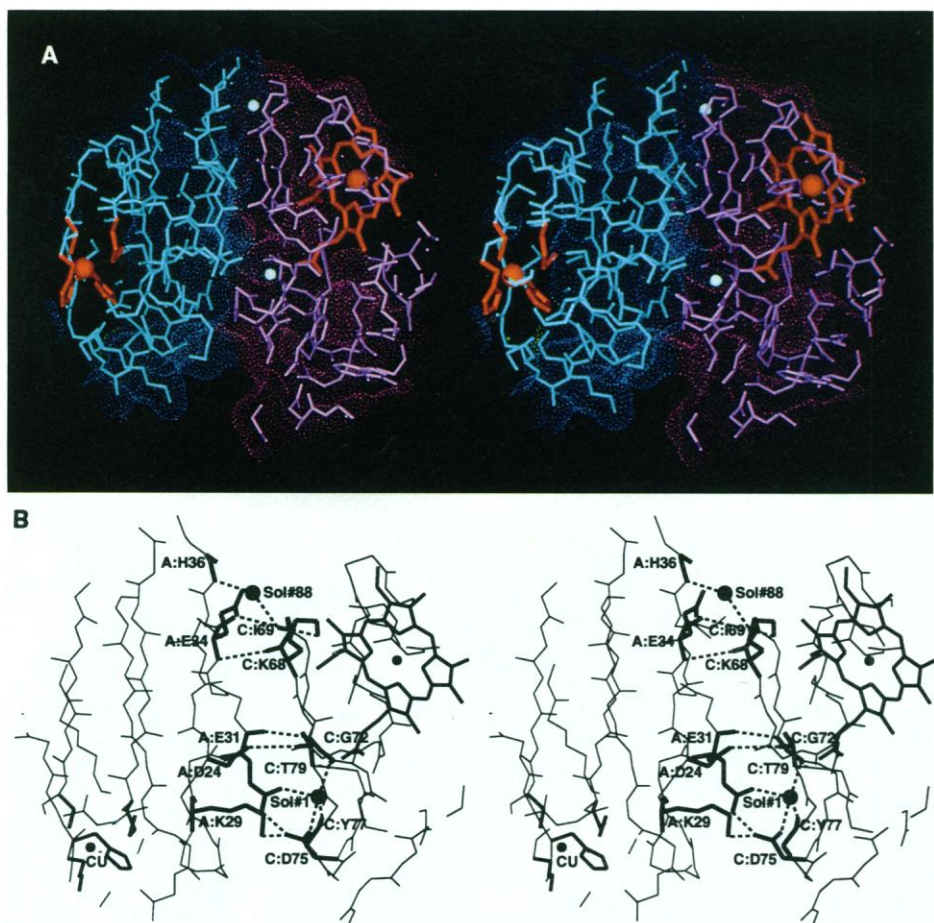


**Fig. 5.** Stereo diagrams of the amicyanin–cytochrome  $c_{551i}$  interface (see Table 1). **(A)** The dots represent the Connolly (27) solvent-exposed surface. The colors are as in Figs. 1 and 4. **(B)** The prefix of each residue name stands for the subunit, A: for amicyanin, C: for cytochrome. Residues involved in ionic and hydrogen bonds are shown in thick lines, and the interactions are indicated by dashed lines. Shown in thin lines are the backbone atoms for other residues. Redox centers (the copper, its ligands, and the heme group) are shown in thick lines. Two solvent molecules (filled circles) involved in the interface are also shown.

The amicyanin–cytochrome  $c_{551i}$  interface (Fig. 5 and Table 1) differs from the MADH-amicyanin interface. It is smaller, occupying about  $420 \text{ \AA}^2$  on amicyanin and about  $445 \text{ \AA}^2$  on the cytochrome, and more polar. Of the 10 amicyanin residues in the interface, 6 are charged (3 positive and 3 negative) and 2 are neutral hydrophilic. Of the 12 interface residues of the cytochrome, 1 is positive, 2 are negative, 3 are neutral hydrophilic, and 6 are hydrophobic. Thus, approximately 64% of the residues in the interface are hydrophilic compared with about 40% in the MADH-amicyanin interface. The number of links between amicyanin and the cytochrome is greater than between amicyanin and MADH, with one salt bridge, four hydrogen bonds, and one Glu-Asp interac-

**Table 1.** Amicyanin–cytochrome  $c_{551i}$  contacts (3.5 Å or less). The prefixes A: and C: refer to amicyanin and cytochrome  $c_{551i}$ , respectively. The following additional residues are contained within the amicyanin–cytochrome  $c_{551i}$  interface on the basis of a decrease in solvent accessibility, but are further than 3.5 Å from the partner molecule: A:Ala<sup>26</sup>, A:Lys<sup>27</sup>, A:Pro<sup>33</sup>, A:His<sup>36</sup>, C:Glu<sup>66</sup>, C:Gly<sup>70</sup>, C:Asn<sup>74</sup>, and C:Ala<sup>76</sup>. In addition to the direct connections between amicyanin and cytochrome  $c_{551i}$ , there is a potential salt bridge between A:Glu<sup>34</sup> and C:Lys<sup>68</sup>. In the crystal structure, both side chains point away from the interface into solution. However, an interaction between them can easily be modeled and might form at lower ionic strength. Of the other charged or neutral groups in the interface, one intramolecular salt bridge between A:Asp<sup>24</sup> and A:Arg<sup>48</sup> and one intramolecular hydrogen bond between A:Glu<sup>34</sup> and A:His<sup>36</sup> lie on the amicyanin surface. The remaining charged or neutral groups point into solution, away from the interface, except for A:Thr<sup>32</sup>, which forms a hydrogen bond to a solvent molecule within the interface.

Amicyanin	Cytochrome $c_{551i}$	Distance (Å)
<i>Van der Waals interactions</i>		
Asp <sup>24</sup> CB	Tyr <sup>77</sup> CE2	3.4
Glu <sup>31</sup> CD	Asp <sup>75</sup> OD1	3.5
Glu <sup>31</sup> O	Pro <sup>71</sup> CA	3.2
Thr <sup>32</sup> CG2	Ile <sup>69</sup> O	3.4
Glu <sup>34</sup> OE1	Ile <sup>69</sup> CD	3.4
Arg <sup>48</sup> NE	Tyr <sup>77</sup> OH	3.4*
<i>Hydrogen bonds</i>		
Asp <sup>24</sup> OD1	Thr <sup>79</sup> OG1	3.4
Glu <sup>31</sup> OE2	Asp <sup>75</sup> OD1	2.7
Glu <sup>31</sup> O	Gly <sup>72</sup> N	3.1
Glu <sup>34</sup> N	Lys <sup>68</sup> O	3.4
<i>Salt bridge</i>		
Lys <sup>29</sup> NZ	Asp <sup>75</sup> OD1	2.9
<i>Bridging solvent molecules</i>		
Sol <sup>1</sup>	A:Glu <sup>31</sup> OE1	2.7
Sol <sup>1</sup>	C:Gly <sup>72</sup> O	2.6
Sol <sup>1</sup>	C:Asp <sup>75</sup> OD2	2.7
Sol <sup>1</sup>	C:Tyr <sup>77</sup> O	2.5
Sol <sup>88</sup>	A:His <sup>36</sup> N	2.9
Sol <sup>88</sup>	A:Ile <sup>69</sup> O	3.0

\*The angle between side chains precludes hydrogen bond formation.

tion, which is possibly stabilized by protonation of one of the side chains or by interaction with a solvent molecule (16). One additional solvent molecule is involved in bridging the subunits.

In considering possible paths for electron flow from TTQ to copper and from copper to iron in the ternary complex, we used the program PATHWAYS-II (17) as a guide. Two prominent paths, predicted by the program, lead to the copper atom from the indole ring of Trp<sup>57</sup>. One utilizes Trp<sup>108</sup> of TTQ whereas the other follows two main chain residues of the L subunit. Calculation of the relative efficiencies of these two paths with PATHWAYS-II indicates that in the latter the coupling is about threefold more efficient than in the former, but depends critically on the presence of a water molecule that might not always be occupied, thereby reducing the relative efficiency of this pathway. In the case of the electron transfer from copper to iron, the two most prominent paths follow either Cys<sup>92</sup> or Met<sup>98</sup>, both of which are copper ligands, to a common point and continue through three residues of amicyanin and two of the cytochrome. PATHWAYS-II calculates both branches to have approximately equal efficiency.

The electronic coupling from copper to iron is less efficient than from TTQ to copper by a factor of  $\sim 10^3$ , on the basis of the PATHWAYS II calculation; this is due in part to the greater overall length of the copper-to-iron paths as compared with the TTQ to copper paths. These calculations lead one to predict that the electron transfer rate from amicyanin to cytochrome  $c_{551i}$  should be six orders of magnitude less than from MADH to amicyanin. This prediction is not, however, realized in solution studies (18), which indicate rates of approximately the same order of magnitude, 10 to 50 s<sup>-1</sup>.

The apparent lack of a direct correlation between electron transfer rate and coupling efficiency is not surprising, because in this complex, unlike many model systems (1), one is not observing an activationless electron transfer (one in which the driving force is approximately equal to the reorganizational energy). The relatively slow electron transfer rate for the reaction between TTQ and copper suggests that this reaction exhibits a large reorganizational energy or that it is a gated process (where one is measuring the rate of a conformational change or solvent reorganization rather than electron transfer) (19). Most naturally occurring biological electron transfer reactions are probably not activationless, having relatively low driving forces compared with the reorganizational energies (1).

The presence of two distinct electron transfer sites on amicyanin is not unexpected. It is consistent with previous studies (8) which showed that all three com-

ponents are required for oxidation of MADH or of amicyanin by cytochrome  $c_{551i}$ , supporting the idea that a ternary complex is formed in solution. Amicyanin is closely related in structure to plastocyanin (20), which also has been observed to have two distinct electron transfer sites. Plastocyanin, a cupredoxin found in chloroplasts, transfers electrons from cytochrome *f* to the chlorophyll P700 of photosystem I. It has a hydrophobic surface patch separated from the copper by 3 to 9 Å and centered on a surface-exposed histidine copper ligand (21). This site appears to be used for interaction with the P700 (22). However, cytochrome *f*, and other cytochromes, appear to utilize a second, remote site some 14 to 19 Å from the copper, centered on a tyrosine, adjacent to the cysteine copper ligand (23). In amicyanin, the counterpart to this tyrosine is His<sup>91</sup>, which is next to the copper ligand Cys<sup>92</sup>. However, access to His<sup>91</sup> by cytochrome  $c_{551i}$  is blocked by MADH in the complex.

Electron transfer studies between plastocyanin and various cytochromes indicate that a structural rearrangement may occur after formation of an initial complex and before the electron transfer event (24). It is possible that the complex between amicyanin and cytochrome  $c_{551i}$ , which we observe in the ternary complex, does not correspond to the optimal geometry for the electron transfer event, and a realignment might be necessary.

## REFERENCES AND NOTES

1. J. N. Onuchic, D. N. Beratan, J. R. Winkler, H. B. Gray, *Annu. Rev. Biophys. Biomol. Struct.* **21**, 349 (1992).
2. C. W. Canters and M. van de Kamp, *Curr. Opin. Struct. Biol.* **2**, 859 (1992); J. W. Evenson and M. Karplus, *Science* **262**, 1247 (1993).
3. V. Davidson, in *Principles and Applications of Quinoproteins*, V. Davidson, Ed. (Decker, New York, 1993), pp. 73–95.
4. L. Chen *et al.*, *Proteins* **14**, 288 (1992). The original determination of the crystal structure of *P. denitrificans* MADH was based on an x-ray sequence derived for the enzyme from *Thiobacillus versutus* [F. M. D. Vellieux, K. H. Kalk, J. Drenth, W. G. J. Hol, *Acta Crystallogr.* **B46**, 806 (1990)]. This structure has been rebuilt with the DNA-derived amino acid sequence [A. Y. Chistoserdov, G. Boyd, F. S. Mathews, M. E. Lidstrom, *Biochem. Biophys. Res. Commun.* **184**, 1181 (1992)] and refined at 1.75 Å resolution [L. Chen *et al.*, unpublished data].
5. W. S. McIntire, D. E. Wemmer, A. Chistoserdov, M. Lidstrom, *Science* **252**, 817 (1991); L. Chen *et al.*, *FEBS Lett.* **287**, 163 (1991).
6. M. Husain and V. L. Davidson, *J. Biol. Chem.* **260**, 14626 (1985); M. Husain, V. L. Davidson, A. J. Smith, *Biochemistry* **25**, 2431 (1986); R. M. J. Van Spanning, C. W. Wansell, W. N. M. Reijnders, F. L. Oltmann, A. H. Stouthamer, *FEBS Lett.* **275**, 217 (1990).
7. L. Chen *et al.*, *Biochemistry* **31**, 4959 (1992). The crystal structure of the binary complex between MADH and amicyanin was based in part on an x-ray sequence for MADH as described in (4).
8. Three periplasmic c-type cytochromes,  $c_{550}$ ,  $c_{551i}$ , and  $c_{553i}$ , have been characterized from methylamine-grown cells of *P. denitrificans* [M. Husain and V. L. Davidson, *J. Biol. Chem.* **261**, 8577 (1986); K. A. Gray, D. B. Knaff, M. Husain, V. L. Davidson, *FEBS Lett.* **207**, 239 (1986)]. It was shown in vitro that these cytochromes may be reduced only in the presence of both MADH and amicyanin, indicating that the cytochrome must react with a complex of MADH and amicyanin. Of these cytochromes, the one that reacts the most efficiently in vitro is cytochrome  $c_{551i}$ .
9. L. Chen *et al.*, *Protein Sci.* **2**, 147 (1993).
10. A. T. Brünger, *X-PLOR Manual, Version 3.0* (Yale University, New Haven, 1992).
11. The refined holo-amicyanin complex has an *R* factor of 0.191 in the resolution range 12.0 to 2.8 Å with rms deviations of 0.019 Å and 3.99°, and contains 5805 protein atoms, one heme group, one copper ion, 90 solvent molecules, and one phosphate in the model. Since the apo and holo structures are not significantly different and the apo-complex data extend to higher resolution, the discussion is based primarily on the coordinates of the apo-amicyanin complex.
12. E. C. Huizinga *et al.*, *Biochemistry* **31**, 9789 (1992).
13. F. S. Mathews, *Prog. Biophys. Mol. Biol.* **45**, 1 (1985).
14. In the crystal lattice, two cytochrome molecules are closely packed about a crystallographic twofold axis parallel to the *b* axis. As a consequence, an interface is formed between them having an area of about 650 Å<sup>2</sup>. It is made up of 18 amino acid residues plus pyrrole ring C of the heme group and is extremely hydrophobic. There are no salt bridges, hydrogen bonds, or water molecules linking the two cytochromes. The two iron atoms are about 18 Å apart, whereas the closest edge-to-edge distance of the two heme groups is about 7 Å.
15. W. Kabsch and C. Sander, *Biopolymers* **22**, 2577 (1983).
16. The environment of this solvent molecule (#1, Fig. 5B) is of special interest. It is coordinated to two acidic side chains, Glu<sup>91</sup> of amicyanin and Asp<sup>75</sup> of the cytochrome, which also interact with each other, and to Gly<sup>72</sup>O and Tyr<sup>77</sup>O of the cytochrome. This solvent was modeled into the highest peak of the difference map, at 9.5σ (the rms electron density), and as water its temperature factor refined to a low value (4.3 Å<sup>2</sup>). Since the solvent is surrounded by four nonprotonated oxygen atoms, it could be a cation such as sodium or potassium. As such, it would help explain the interaction between Glu<sup>91</sup> of amicyanin and Asp<sup>75</sup> of the cytochrome through partial neutralization of their negative charges.
17. J. J. Regan, PATHWAYS II, Version 2.01 (San Diego 1993).
18. The electron transfer rate from substrate-reduced MADH to amicyanin was determined from stopped-flow experiments to be 24 s<sup>-1</sup> at 20°C [H. B. Brooks and V. L. Davidson, *Biochem. J.* **294**, 211 (1993)], whereas from dithionite-reduced MADH to amicyanin it varied from ~2 to 55 s<sup>-1</sup> over a temperature range of 10° to 50°C [H. B. Brooks and V. L. Davidson, unpublished results]. A minimum value for the electron transfer rate from copper to iron may be inferred from steady-state kinetic experiments. The  $k_{cat}$  (per site) for the methylamine-dependent reduction of cytochrome  $c_{551i}$  by the MADH and amicyanin is about 9 s<sup>-1</sup> at 30°C [V. L. Davidson and L. H. Jones, *Anal. Chim. Acta* **249**, 235 (1991)]. No individual rate constant for this overall reaction, including the rate of electron transfer from amicyanin to cytochrome, can be less than  $k_{cat}$ .
19. B. M. Hoffman and M. A. Ratner, *J. Am. Chem. Soc.* **109**, 6237 (1987).
20. R. Durley, L. Chen, L. W. Lim, F. S. Mathews, V. L. Davidson, *Protein Sci.* **2**, 739 (1993).
21. J. M. Guss and H. C. Freeman, *J. Mol. Biol.* **169**, 521 (1983).
22. M. Nordling, K. Sigfridsson, S. Young, L. G. Lundberg, O. Hansson, *FEBS Lett.* **291**, 327 (1991).

23. S. He, S. Modi, D. S. Bendall, J. C. Gray, *EMBO J.* **10**, 4011 (1991).  
 24. T. E. Meyer, Z. G. Zhao, M. A. Cusanovich, G. Tollin, *Biochemistry* **32**, 4719 (1993); L. M. Peerey, H. M. Brothers, J. T. Hazzard, G. Tollin, N. M. Kostic, *ibid.* **30**, 9297 (1991); L. Qin and

- N. M. Kostic, *ibid.* **32**, 6073 (1993).  
 25. Coordinates for the ternary complex have been deposited in the Brookhaven Protein Data Bank (entry code 2MTA).  
 26. P. J. Kraulis, *J. Appl. Crystallogr.* **24**, 946 (1991).

27. M. Connolly, *ibid.* **16**, 548 (1983).  
 28. We thank A. G. Mauk and G. Tollin for helpful comments. Supported by NSF grant MCB-9119789 (F.S.M.) and by USPHS grant GM41574 (V.L.D.).

12 October 1993; accepted 16 February 1994

## Neutrophil Activation by Monomeric Interleukin-8

Krishnakumar Rajarathnam, Brian D. Sykes, Cyril M. Kay, Beatrice Dewald, Thomas Geiser, Marco Baggiolini, Ian Clark-Lewis\*

Interleukin-8 (IL-8), a pro-inflammatory protein, has been shown by nuclear magnetic resonance (NMR) and x-ray techniques to exist as a homodimer. An IL-8 analog was chemically synthesized, with the amide nitrogen of leucine-25 methylated to selectively block formation of hydrogen bonds between monomers and thereby prevent dimerization. This analog was shown to be a monomer, as assessed by analytical ultracentrifugation and NMR. Nevertheless, it was equivalent to IL-8 in assays of neutrophil activation, which indicates that the monomer is a functional form of IL-8.

Interleukin-8 is an inflammatory cytokine that promotes the accumulation and activation of neutrophil leukocytes (1) and has been implicated in a wide range of acute and chronic inflammatory diseases (2). In vitro, IL-8 induces neutrophil shape change, chemotaxis, granule release, and respiratory burst (1) by binding to receptors of the seven transmembrane segment class (3). The structure of human IL-8, as solved by NMR and x-ray methods (4, 5), shows a noncovalent homodimeric topology (Fig. 1). The dimer interface is formed by a  $\beta$  strand from each monomer and by part of the  $\alpha$  helices that lie across the  $\beta$  sheet formed on dimerization. The principal interactions stabilizing the dimer are the six H bonds involving Leu<sup>25</sup>, Val<sup>27</sup>, and Glu<sup>29</sup>. The NH<sub>2</sub>-terminal residues Glu<sup>4</sup>, Leu<sup>5</sup>, and Arg<sup>6</sup> are essential for neutrophil activation in vitro (6, 7), although other structural features are also important (6). However, the COOH-terminal  $\alpha$  helix was not essential for activity, which suggests that the groove between the helices is not a critical binding site.

Many growth factors are di- or trimeric, although the functional conformation may not correspond to the observed form, as structure determinations are done at higher concentrations than those in the biological-

ly effective range. Nevertheless, receptor aggregation is a requirement for the signaling of some receptors (8), and cross-linking mediated by the ligand has been demonstrated in some instances (9).

Our aim was to obtain a monomeric form of IL-8. Conventional amino acid replacement results in changes in the chemical nature of the amino acid side chains but does not necessarily affect the dimeric structure. Our approach was to selectively disrupt the secondary structure that stabilizes the dimer interface by modification of the peptide backbone. This could be achieved by site-directed mutagenesis or chemical synthesis (10). Because IL-8 can be readily synthesized chemically (11), this method was used to obtain an analog in which the amide of Leu<sup>25</sup>, which is normally involved in H bonding across the dimer interface, is methylated (NH  $\rightarrow$  NCH<sub>3</sub>) (12). This analog (L25NMe) induced neutrophil chemotaxis

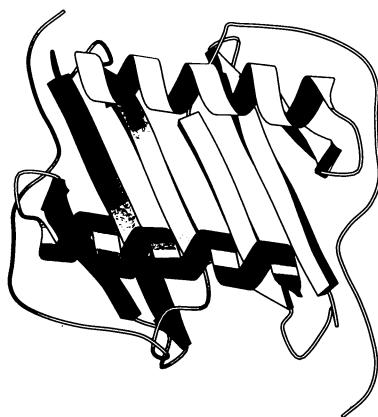


**Fig. 1.** A schematic diagram of IL-8 generated with the program MOLSCRIPT (19) which used the coordinates of the NMR structure (4).

(Fig. 2A) and the release of elastase (Fig. 2B), as well as the respiratory burst and the mobilization of cytosolic free calcium (13), and competed with labeled IL-8 for binding to the IL-8 receptors (Fig. 2C). In all the assays, the activities of L25NMe and IL-8 were similar. The sedimentation equilibrium profiles (Fig. 3) of the L25NMe analog and of IL-8 corresponded to those expected for a monomer and a dimer, respectively (14). No evidence for higher order aggregates was found for either form.

In NMR studies, relatively large (>0.3

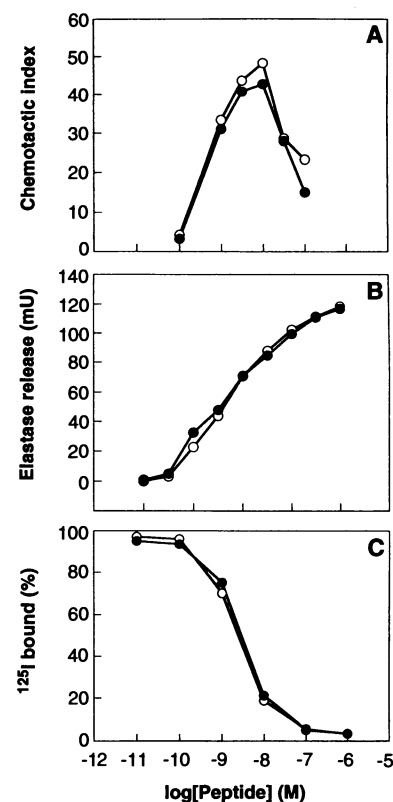


**Fig. 2.** Biological activities of the L25NMe analog (●) and IL-8 (○) on human neutrophils as assessed by (A) chemotaxis, (B) elastase release, and (C) receptor binding. The chemotactic index is the ratio of neutrophils that migrated in the presence or absence of chemoattractant and elastase release is expressed as milliunits (mU) of enzyme activity (20). Displacement of <sup>125</sup>I-labeled IL-8 by unlabeled IL-8 or L25NMe was determined as described (21). All measurements were done in duplicate at various molar concentrations (M) of peptide. All the assays were done at least three times, with concentrations were calculated from the measured weight of the lyophilized material and the molecular weight of the monomer.

K. Rajarathnam, B. D. Sykes, C. M. Kay, Protein Engineering Network of Centres of Excellence (PENCE) and Department of Biochemistry, 713 Heritage Building, University of Alberta, Edmonton, Alberta, Canada T6G 2S2.

B. Dewald, T. Geiser, M. Baggiolini, Theodor-Kocher Institute, University of Bern, Post Office Box 99, CH-3000 Bern, Switzerland.

I. Clark-Lewis, Biomedical Research Centre, Department of Biochemistry and Molecular Biology, and PENCE, University of British Columbia, Vancouver, British Columbia, Canada V6T 1Z3.

\*To whom correspondence should be addressed.